Environmental Chemistry Letters (2019) 17:465–472
https://doi.org/10.1007/s10311-018-0774-z

ORIGINAL PAPER

Amino acid-imprinted polymers as highly selective CO_2 capture materials

Sreedipta Chaterjee[1] · **Reddithota J. Krupadam**[1]

Received: 3 May 2018 / Accepted: 28 June 2018 / Published online: 12 July 2018

Abstract

The recent atmospheric concentration of CO_2 increase to 400 ppm is a cause of global climate change. There is therefore an urgent need for selective and cost-effective CO_2 capture technologies. Fossil fuel consumption during energy production and transportation are two major sources of CO_2 emission into the atmosphere. The capture of CO_2 selectively from gaseous mixtures using reusable adsorbent is thus a challenge. In this article, we report that nanoparticles functionalized with imprinting of amino acids exhibit a significant increase in the selective adsorption capacities of CO_2 in a gaseous mixture. Molecular imprinting of taurine in the vinylbenzyl chloride-*co*-divinyl benzene polymer formed cavities of 1–3 nm size and introduced –SOOH and –N–H functionalities, resulting in a very high CO_2 adsorption capacity of 5.67 mmol g^{-1} at 30 °C/1 bar. The selectivity of CO_2 over N_2 and CH_4 was 87–91% and 83–87%, respectively. The isosteric heat of adsorption (Q_{st}) for CO_2 at 298 and 303 K showed an increase in Q_{st} from 36.8 to 47.6 K kJ mol^{-1}, and this would be responsible for high CO_2 adsorption energies and faster kinetics. This study reports first-time imprinting of CO_2-philic templates in the polymers to capture small gas molecules at ambient conditions, and the results demonstrated that the polymers have a wide scope for real-life applications of CO_2 capture.

Keywords Carbon dioxide capture · Adsorbents · Selective CO_2 adsorption · Molecular imprinting · Nanoporous polymers

Introduction

Since 1970, the atmospheric CO_2 concentration has steadily increased from 310 to 400 ppm. The responsible factors for such sharp rise in CO_2 concentration are industrial stacks and fugitive emissions, auto exhausts, thermal power stations, natural wetlands and ruminates. The single largest source of CO_2 emission is thermal power plants (Edenhofer 2011). During the past decade, different kinds of dry adsorbents such as zeolites, metal–organic frameworks and microporous organic polymers have been explored as alternatives to the current commercial absorption technology (Xu and Hedin 2014; Abanades et al. 2015). In designing solid adsorbents for CO_2 capture, the adsorbents should have (1) an adsorption capacity greater than 3.0 mmol g^{-1} at pressure 1 bar/temperature between 313 and 353 K, (2) reasonable rate of CO_2 adsorption, and (3) high selectivity toward CO_2. Some of the classical examples of polymer adsorbents reported in the literature are: (1) Hyper-cross-linked polymers containing tetraphenylmethane showed CO_2 adsorption capacity of 2.5 mmol g^{-1}; and the hyper-cross-linked polymers formulated with binaphthol reported CO_2 adsorption capacity of 4.00 mmol g^{-1} (Errahali et al. 2014). (2) Benzimidazole-linked showed very good CO_2 uptake, i.e., 5.34 mmol g^{-1} at 1.0 bar (Altarawneh et al. 2014). (3) Poly (melamine-formaldehyde) materials showed a CO_2 uptake capacity of 4.54 mmol g^{1} at 273 K (Tan et al. 2013). (4) A coordination polymer network with exceptional CO_2 uptake (5.54 mmol g^{-1}) is reported (Choi and Suk 2009).

The high-adsorption-capacity adsorbents with non-selectivity restrict application of adsorbents for real-life situations. The non-selective materials are difficult to regenerate, and the adsorbed gases cannot be reused due to the presence of non-targeted gases. For example, stack emissions from thermal power plants contain 14–16% CO_2, 75–80% N_2 and 10% other gases. Such situations demand precisely designed materials with exceptionally high capability to recognize target molecule in complex mixtures/matrices. Adsorbents

✉ Reddithota J. Krupadam
rj_krupadam@neeri.res.in

[1] Environmental Impact and Sustainability Division, CSIR-National Environmental Engineering Research Institute, Nehru Marg, Nagpur 440020, India

prepared with metal ions and organic linkers emerged as highly selective CO_2 adsorption adsorbents at ambient conditions (Li et al. 2013). Lu et al. (2011) developed a group of high-surface-area polymers by grafting with sulfonic acid and its lithium salt exhibited high selective CO_2 adsorption capacities. The iminebenzothiazole polymer prepared via Schiff's base condensation reaction showed good CO_2 uptake (7.8 wt% at 273 K/1 bar). The polymer also reported selectivity for CO_2 in the gaseous mixtures N_2 (51) and CH_4 (6.3) (Rabbani et al. 2017). The benzimidazole-linked polymers are another group of adsorbents that showed CO_2 selectivity in the presence of N_2 (70) and H_2 (10) (Zhu et al. 2013a, b). McDonald et al. (2014) reported CO_2 capture by amino acid ionic liquids, and impact of water on CO_2 capture. The ionic liquids—tetramethylammonium glycinate ([N1111][Gly]) and tetraethylammonium prolinate ([N2222] [Pro])—with CO_2 under wet conditions form carbamate by the amine-functionalized anions of these salts. By adding CO_2 to these salts, the carbamate releases the covalently bound CO_2. Liu et al. (2018) reported 3D network structures of nanofibers of hydrogels with adsorption capacity of 1.78 mmol g^{-1} and regenerable for about 10 times.

Another desired parameter of adsorbents for real-life application is thermodynamic efficiency of regeneration. Polyethyleneimine adsorbents are regenerable; however, formation of carbamate reduces the adsorbent performance in thermal swing regeneration (Drage et al. 2009). Triazine-based benzimidazole-linked polymers showed CO_2 uptake capacity (5.19 mmol g^{-1}) (Sekizkardes et al. 2014). The porous azo-linked polymers showed high CO_2 uptake of 5.37 mmol g^{-1}, and these polymers reported Q_{st} values (28–30 kJ/mol) for CO_2 capture (Arab et al. 2015).

Our earlier studies report that the naturally occurring solid amino acids with CO_2-philic functionality are good candidates of CO_2 adsorption (Chatterjee et al. 2016). In this study, the polymer has been imprinted with amino acid taurine to increase surface area considerably, and the cavities are decorated with CO_2-philic functionalities. The size of the cavities in the polymer ranges between 1 and 3 nm. The size of CO_2 is 0.21 nm, and the pores with size 1.0 nm are desired for effective CO_2 adsorption (Wilmer et al. 2012; Hudson et al. 2012). It is also presumed that the Q_{st} for CO_2 can be improved by incorporating polar functionality of amino acids that interact with CO_2.

Experimental

Chemicals

Vinylbenzyl chloride and divinylbenzene were purchased from Sigma-Aldrich (St. Louis, USA). Amino acid taurine and the solvents dichloromethane and acetonitrile were purchased from Merck (Potsdam, Germany). High-purity (99.999%) gases CO_2, N_2 and CH_4 were purchased from Nikhil Gases (Nagpur, India). Helium high-purity gas was used as the purge gas in simultaneous thermal analyzer during CO_2 adsorption–desorption experiments. All other chemicals were used as purchased.

Preparation of amino acid-imprinted and non-imprinted polymers

The hyper-cross-linked polymers prepared with the composition of vinylbenzylchloride (VBC) and divinylbenzene (DVB) reported high surface area (Errahali et al. 2014), and the same composition is used in imprinting of taurine to create CO_2-philic functionality. This is a new approach to create specific functionality in high-surface-area polymers. The imprinted polymers were prepared using the composition given in Table 1. The procedure followed for synthesis of the non-imprinted polymer is described in Krupadam et al. (2014). Briefly, the polymer precursors with DVB given in Table 1 were heated to 340 K for about 8 h under nitrogen, and the polymerization was controlled with methanol. The polymer monolith was separated from the solvent by filtration, and the monolith was thoroughly washed with methanol. Using analytical ball mill, the polymeric monolith was made into fine particles of size between 70 and 100 µm. The polymer particles were cleaned by Soxhlet extraction

Table 1 Polymer composition and surface properties

Polymer	Polymer composition				Surface properties		
	FM, DVB [mmol (mg)]	X-L, VBC [mmol (mg)]	*T* [mmol (mg)]	Solvent (mL)	SA_{BET} (m^2 g^{-1})	APV (cm^3 g^{-1})	APD (Å)
Non-imprinted polymer	4.0 (0.53)	20 (30.6)	0	100	1020	0.316	13
Imprinted polymer	4.0 (0.53)	20 (30.6)	1 (0.13)	100	650	0.059	56

P polymer, *IP* imprinted polymer, *FM* functional monomer, *DVB* divinylbenzene, *X-L* cross-linking monomer, *VBC* vinylbenzylchloride, *T* template (taurine, an amino acid), SA_{BET} Brunauer–Emmett–Teller (BET) surface area, *APV* average pore volume, *APD* average pore diameter

using methanol for 24 h and then dried in vacuum at 70 °C overnight. The other polymer, imprinted polymer, was prepared by following the same procedure; however, taurine was added before the addition of formaldehyde dimethyl acetal (FDA) and $FeCl_3$. After polymerization, taurine was removed from the polymer using Soxhlet extraction using methanol for 24 h, and then, water was used as the solvent for Soxhlet extraction for another 24 h. After the removal of template, the polymer was dried in vacuum at 70 °C overnight. These polymers were used for adsorption of CO_2 and other gases.

Characterization of polymers

Surface area, pore volume and average pore diameter of the polymers were determined using N_2-adsorption isotherms in Micromeritics ASAP 2420 at 77 K. Nitrogen adsorption surface area of IP was computed by Brunauer–Emmett–Teller equation (Walton and Snurr 2007), and pore volumes were calculated from the Dubinin–Radushkevich equation based on N_2-adsorption isotherms (Carrasco-Martin et al. 1993). Polymers prepared were kept under vacuum at 373 K for about 7 h. Surface topology of the polymers was viewed using atomic force microscope (FlexAFM, Nanosurf AG, Switzerland). Tapping tips were procured from Silicon AFM Probes (Tap 300, Ted Pella, Inc) whose resonant frequency was between 290 and 410 kHz. The micrograph of the imprinted polymer was analyzed with Easyscan 2 Software. Furthermore, laser Raman microscope (Alpha 300 RA, WITec, Germany) equipped with a frequency-doubled Nd:YAG laser for 532 nm excitation to observe morphology of the polymers. The Raman imaging was integrated with spectral lines of CH_2 stretching using 1 s with accumulation of 10. The measurements were acquired using the WITec Control Software. The attenuated total reflectance infrared spectra of polymers were recorded on a Digilab FTS equipped with an HgCdTe detector. The wave numbers scan ranges from 600 to 4000 cm with 4 cm^{-1} of spectral resolution.

CO_2 adsorption experiments

The adsorption experiments for CO_2 adsorption and desorption were conducted in a simultaneous thermal analyzer (STA; PerkinElmer 6000), and the detailed procedure is reported in our earlier article (Chatterjee et al. 2016). The adsorption isotherms were drawn at 273 and 303 K at different pressures (up to 10 bar). After adsorption of CO_2, the adsorbed CO_2 was flushed with He gas at 473 K for 5 min. Once the polymer was degassed, CO_2 gas was passed till saturation to record the adsorption capacity. These adsorption–desorption cycles were repeated for 50 cycles. For selectivity measurements, equimolar concentration of gaseous mixtures (CO_2 and N_2; and CO_2 and CH_4) was passed through the simultaneous thermal analyzer. The Q_{st} of CO_2 was measured in the Micromeritics ASAP 2420, and data from the adsorption isotherm were also used.

Results and discussion

Molecular imprinting is used to create molecule-specific cavities in terms of both geometry and functionality in the polymer to selectively recognize and capture the targeted molecule (Wulff 1995). In this study, molecular imprinting technique was used to create cavities of size between 1 to 3 nm, and these cavities are decorated with CO_2-philic functionality in the polymers. Earlier reports indicate that pores bigger than 5 times of the adsorbate molecular size are required criteria for effective adsorption of gases, and this conclusion was derived from the study of mathematical simulations by Salles et al. (2008). The molecular size of CO_2 is 0.21 nm, and the pores with size less than 1.0 nm are required for CO_2 adsorption (Wahby et al. 2010). The introduction of CO_2-philic functional groups improves the Q_{st}, which influences capacity and selectivity of adsorbents for CO_2. Banerjee et al. (2009) reported a drastic increase in Q_{st} of CO_2/N_2 adsorption selectivity by introducing polar functionalities; however, this procedure reduces the surface area of the adsorbents significantly. The probable strategy to address this issue is to use high-surface-area polymers as the base materials, and then, the surfaces can be functionalized with CO_2-philic functional groups. The vinylbenzyl chloride-*co*-divinylbenzene polymer was imprinted with taurine which forms small pore (size 1–3 nm) with sulfonate and amine functionalities. Such specific imprinted pores selectively adsorb CO_2 compared to N_2 and CH_4 in gaseous mixtures.

The adsorption of N_2 was performed at 273 K to evaluate the existence of permanent porosity and nature of isotherms of imprinted and non-imprinted polymers. The adsorption isotherms are type I, and the imprinted polymer has permanent microporosity (Fig. 1a). Hence, imprinted polymer showed rapid N_2 adsorption at low pressures. Adsorption isotherms of CO_2 for imprinted and non-imprinted polymers have been plotted for 273 and 303 K, at different pressures up to 1 bar (Fig. 1b). The CO_2 adsorption capacity of imprinted polymer is compared with other adsorbents such as porous polymers (6.0 mmol g^{-1}) (Popp et al. 2015), benzimidazole-linked polymers (5.3 mmol g^{-1}) (Zhu et al. 2013a, b) and Tröger's base-derived covalent organic polymers (5.16 mmol g^{-1}) at 273 K (Byun et al. 2014). It would be clear from the adsorption isotherms that the taurine-imprinted polymer has the functionality of amine and sulfonic acid in the micro/nanocavities. Infrared spectra of the imprinted polymer before and after adsorption of

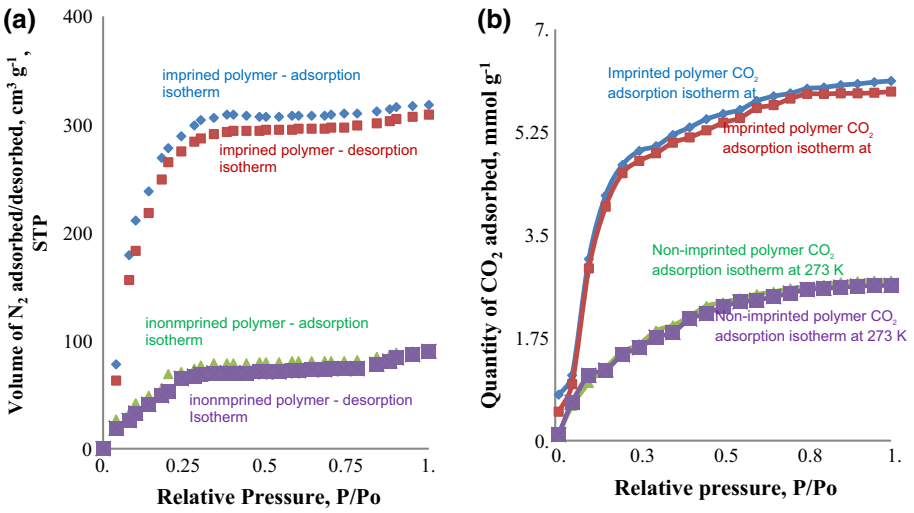

Fig. 1 Gas adsorption and desorption isotherms **a** N_2 adsorption and desorption isotherms of imprinted and non-imprinted polymers at 273 K and **b** CO_2 adsorption and desorption isotherms of imprinted and non-imprinted polymers at 273 and 303 K. The adsorption isotherms are type I which represents that imprinted polymers contain permanent micro/nanoporosity. The adsorption capacity of imprinted polymer for CO_2 is 5.67 mmol g^{-1} at 303 K

CO_2 provide further evidence of role of taurine-imprinted polymer (Fig. 2a). The stretching vibrations of functional groups, $–CH_2$ and –CH, in the polymer showed peaks 2900 and 2850 cm^{-1} that correspond to C=C stretching vibration in the aromatic ring of divinylbenzene and vinylbenzyl chloride of the non-imprinted polymer. A quite small band at 1260 cm^{-1} corresponds to C–Cl stretching in vinylbenzyl chloride. The –S=O functionality peak at 1190 cm^{-1} and peaks at 1410 and 1510 cm^{-1} for –C–N (stretch) and –N–H (bend) are due to taurine functionality left during molecular imprinting (Ohno et al. 1992). The decrease in peak intensity at 1190, 1410 and 1510 cm^{-1} after adsorption of CO_2 would be seen. Furthermore, laser Raman microscopy provided clear evidence of existence of nanocavities created during taurine imprinting in the polymer, and also the Raman spectra of the polymer shows the specific functionality of –C–S–, –C–N–, –C–O– and $–CH_2$ vibrational spectra at 1080, 1610, 1760 and 2970 cm^{-1}, respectively, evidenced taurine imprinting (Fig. 2b).

Morphologically, the size of imprinted pores is about 5 times higher than that of CO_2 (0.209 nm) which could be another probable reason to retain CO_2 molecules in the pores followed by forming number of double and multiple interactions between the polymer pore functionality and CO_2. The IP showed surface area of 1020 ± 10 m^2 g^{-1} and pore volume 0.316 cm^3 g^{-1} compared with P (non-imprinted polymer). The size distribution curves were calculated by non-local density functional theory (Jagiello and Olivier 2009), where the median value of the pore size of taurine-imprinted polymers was 1 nm. An increase in the surface area 370 m^2 g^{-1} was noticed due to molecular imprinting of taurine. As shown in Table 1, the total pore volume of imprinted polymer was 0.316 cm^3 g^{-1} which is considerably more compared with porous polymer networks (0.07 cm^3 g^{-1}), hyper-cross-linked polymer (0.08 cm^3 g^{-1}) and molecularly imprinted polymers (0.067 cm^3 g^{-1}) (Zhao et al. 2012). The pores formed in the non-imprinted polymer were larger (average pore diameter 40 nm) than the pores in the imprinted polymer (average pore diameter, 1 nm); this lower pore diameter in imprinted polymer would be responsible for increase in surface area and pore volume (Fig. 2c). The morphology of imprinted polymer has been viewed using atomic force microscope. The external surface of this polymer is seen to be a continuous distribution of micro/nanocavities (Fig. 2d). Remarkably, at 273 K, imprinted polymer adsorbs 5.67 mmol g^{-1} of CO_2; this quantity is about 40% higher than the hyper-cross-linked polymers formulated with bis(chloromethyl) monomers (Fontanals et al. 2015).

Practically, the fuels combusted in thermal power plants emit flue gases at ambient conditions typically containing CO_2 concentration which is lower than 15%. Similarly, natural gas reservoirs constitute about 20% of CO_2 and 80% of CH_4. Such instances require selective CO_2 separation from CH_4 and other gases which is a challenging task to provide clean fuel and reusable CO_2. The selective adsorption of CO_2 from the gaseous mixture under low thermodynamic conditions is a great challenge. In this study, imprinted and non-imprinted polymers were used to evaluate the selectivity toward CO_2 in the presence of N_2 and CH_4. The performance of imprinted polymer for uptake of CO_2 in the presence of N_2 and CH_4 is depicted in Fig. 3a. The imprinted polymer showed significantly higher selectivity and capacity compared with P, which would be due to small pore size and functionality created in the imprinted sites. Compared to non-imprinted polymer, the pore diameter of imprinted polymer is quite small (i.e., 1 nm) and would be the cause of high-selectivity adsorption of CO_2. The selectivity of imprinted polymer at 303 K and 10 bar for the adsorption of CO_2 in the presence of N_2 and CH_4 is 91 and 87%, respectively. The selectivity reported by the imprinted polymer is better than the high-selectivity materials reported in the literature such as benzimidazole-linked polymers (Popp

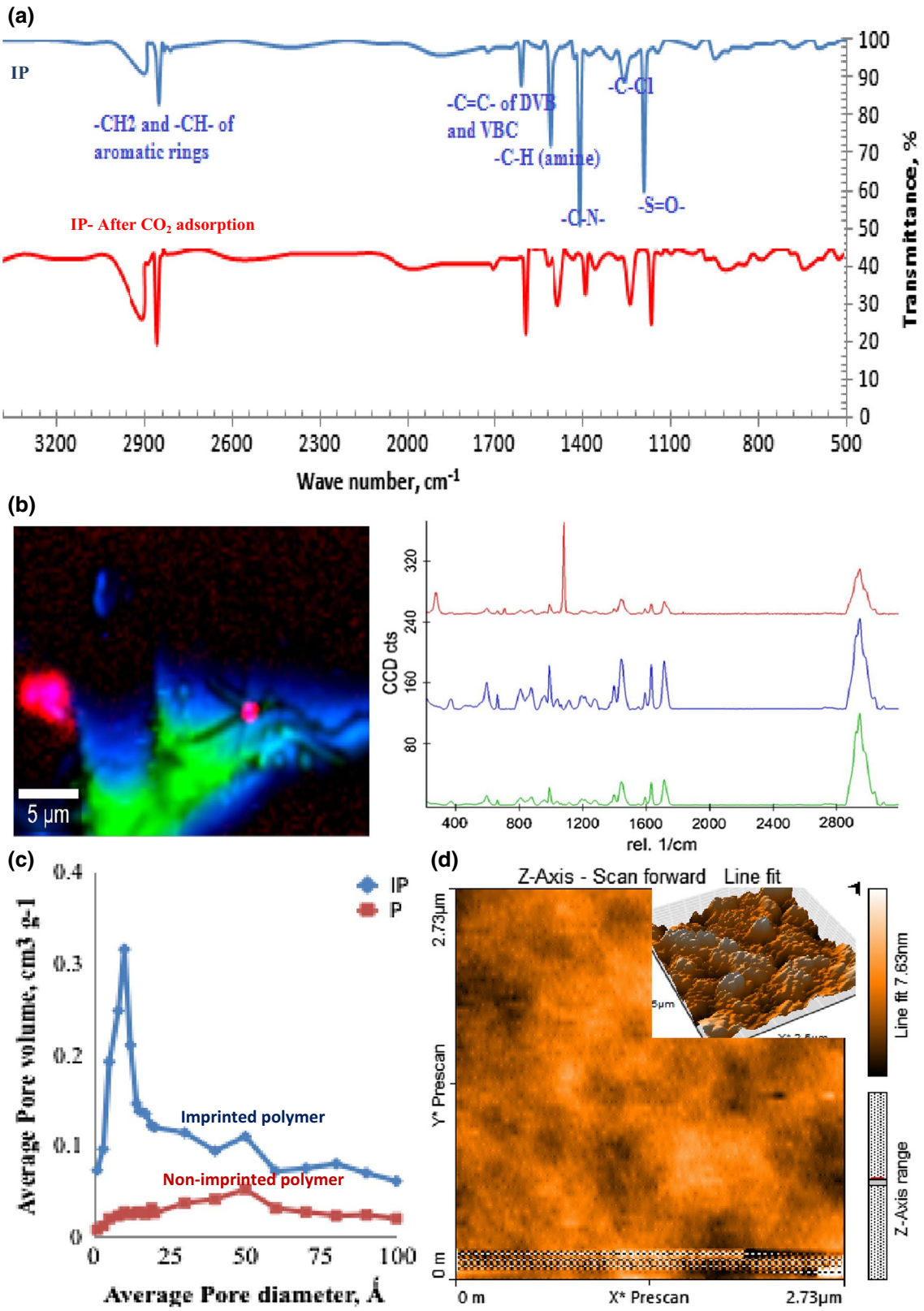

Fig. 2 **a** Infrared spectra, **b** Raman image with spectra, **c** pore size distribution in imprinted and non-imprinted polymers and **d** atomic force microscope image of imprinted polymer (inset: 3D view showing the existing imprinted cavities in the polymer)

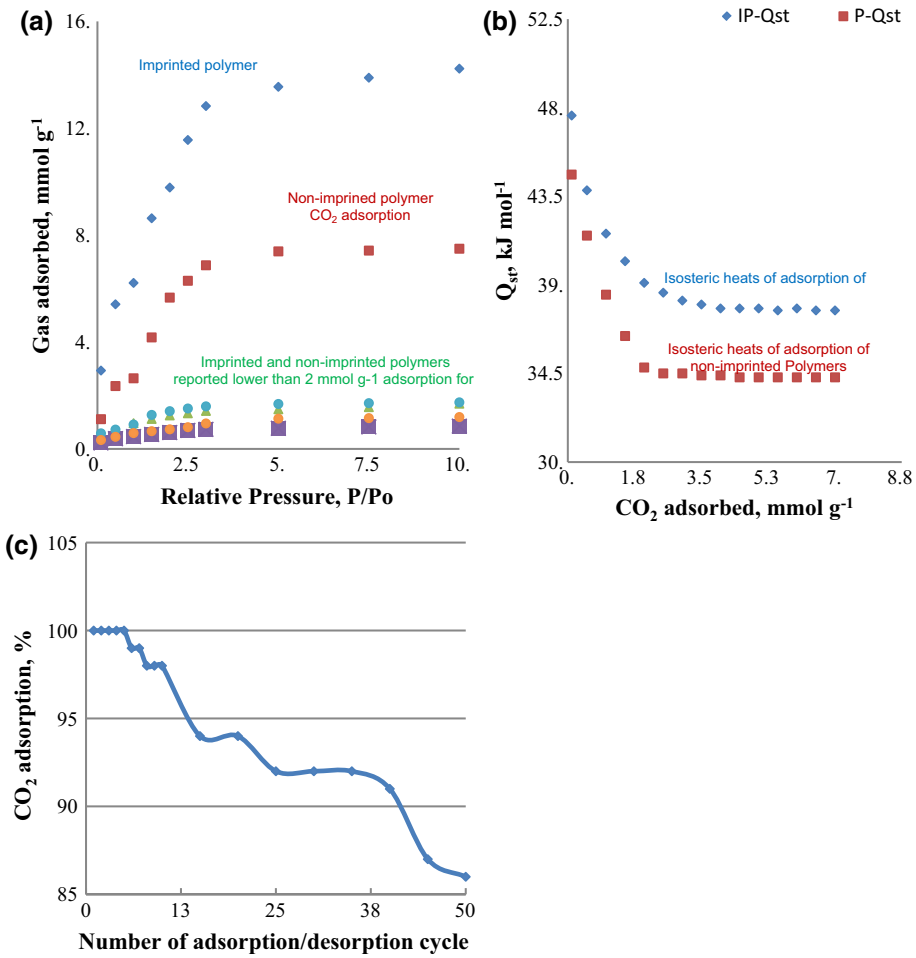

Fig. 3 **a** Adsorption capacity of imprinted and non-imprinted polymers for CO_2, N_2 and CH_4, **b** isosteric heat of adsorption for CO_2 calculated from the isotherms measured at 273 and 303 K for imprinted and non-imprinted polymers and **c** CO_2 adsorption after regeneration of imprinted polymer

et al. 2015). The benzimidazole-linked polymers with the highest CO_2 adsorption showed lowest selectivity (CO_2/N_2, 32:1). With the surface area 1020 $m^2\ g^{-1}$, imprinted polymer showed a significant CO_2 adsorption at 1 bar and 273 K (up to 5.67 mmol g^{-1}); however, the CO_2 adsorption at 10 bar by the imprinted polymer was 26.3 mmol g^{-1}. The high CO_2 adsorption at low pressure could be due to well-formed pore in imprinted polymer which condenses more CO_2 molecules in the polymer. When compared with 3D coordination polymers, the imprinted polymer showed lower adsorption of CO_2 at high pressures. This would be due to the existence of vacant space in 3D-coordinated polymer and other such materials (Choi and Suk 2009).

The isosteric heat of adsorption (Q_{st}) is an indicative of adsorption equilibrium achieved under controlled conditions such as pressure and temperature for a given adsorbate. The Q_{st} of adsorption of polymer was calculated form Langmuir isotherm fits of CO_2 adsorption at 273 and 303 K. The Q_{st} value calculated for CO_2 adsorption for imprinted polymer was 39.8 kJ mol^{-1}, which represents that CO_2 uptake by imprinted polymer was predominantly by physical adsorption. Figure 3b shows a plot of Q_{st} as a function of CO_2 capture. The presence of sulfur and nitrogen atoms in the polymer would be responsible for reduction in the Q_{st} value (4.0 kJ mol^{-1}), thereby improving the affinity toward CO_2 of imprinted polymer compared with non-imprinted polymer. Initially, the Q_{st} was decreased and then stabilized with the CO_2 uptake which represents that imprinted sites with high energy are filled initially, and then reached a saturation level after adsorption of CO_2 to a certain amount. It is important to observe the existence of amine and sulfonic acid functionalities in the imprinted cavities of imprinted polymer that had showed slightly higher Q_{st} which represents stronger CO_2 interaction with imprinted polymer compared with non-imprinted polymer. The heat of adsorption Q_{st} of imprinted polymer is higher than the microporous polycarbazoles (27–31 kJ mol^{-1}) or benzimidazole-linked polymers (20–27 kJ mol^{-1}) or conjugated microporous polymers (25–33 kJ mol^{-1}) or hyper-cross-linked polymers (20–24 kJ mol^{-1}) (Martin et al. 2011; Zhu et al. 2013a, b). The Q_{st} values of imprinted polymer are below 50 kJ mol^{-1}, the interaction between CO_2 and polymers are reasonably weak, and this facilitates regeneration of polymers with quite low energy.

Regeneration of adsorbent is an important aspect which influences the affordability, and multiple cycles of use reduces the cost of CO_2 capture (Abanades et al. 2004). The regeneration of imprinted polymer was evaluated in simulated temperature and pressure-controlled ASAP 2020 analyser. It was found that even after 50 cycles, there was no considerable change in capacity (Fig. 3c). The imprinted polymer reported lower regeneration energies compared to amine solutions. The polymer designed with synergistic approach of hyper-cross-linking and molecular imprinting has high potential for commercial applications due to its selective adsorption of CO_2 and physical–chemical robustness and stability.

Conclusion

In conclusion, taurine-imprinted polymer formulated with divinylbenzene and vinyl benzyl chloride showed high adsorption capacity of 5.67 mmol g^{-1} and selectivity. Furthermore, the adsorbent showed no apparent loss in the CO_2 adsorption capacity till 50 cycles. The polymer prepared using molecular imprinting of CO_2-philic templates demonstrated applicability of adsorbents for real-life CO_2 capture applications. Further studies are underway to establish physical–chemical robustness and stability under different industrially relevant conditions.

Acknowledgements The financial support of the Ministry of Science and Technology, Government of India, under National Program on Carbon Capture and Sequestration Research [Grant No. DST/IS-STAC/CO_2-SR-162/13(G)] is acknowledged.

References

Abanades JC, Rubin ES, Anthony EJ (2004) Sorbent cost and performance in CO_2 capture systems. Ind Eng Chem Res 43:3462–3466. https://doi.org/10.1021/ie049962v

Abanades JC, Arias B, Lyngfelt A, Mattisson T, Wiley DE, Li H, Ho MT, Mangano E, Brandani S (2015) Emerging CO_2 capture systems. Int J Green Gas Control 40:126–166. https://doi.org/10.1016/j.ijggc.2015.04.018

Altarawneh S, Behera S, Jena P, El-Kaderi HM (2014) New insights into carbon dioxide interaction with benzimidazole-linked polymers. Chem Commun 50:3571–3574. https://doi.org/10.1039/C3CC45901B

Arab P, Parrish E, Islamoglu T, El-Kaderi HM (2015) Synthesis and evaluation of porous ago-linked polymers for carbon dioxide capture and separation. J Mater Chem A 3:20586–20594. https://doi.org/10.1039/C5TA04308E

Banerjee R, Furukawa H, Britt D, Knobler C, O'Keefee M, Yaghi OM (2009) Control of pore size and functionality in isoreticular zeolitic imidazolate frameworks and their carbon dioxide selective capture properties. J Am Chem Soc 131:3875–3877. https://doi.org/10.1021/ja809459e

Byun J, Je SH, Patel HA, Coşkun A, Yavuz CT (2014) Nanoporous covalent organic polymers incorporating Troger's base functionalities for enhanced CO_2 capture. J Mater Chem A 2:12507–12512. https://doi.org/10.1039/C4TA00698D

Carrasco-Martin F, Lopez-Ramon MV, Moreno-Castilla C (1993) Applicability of the Dubinin–Radushkevich equation to carbon dioxide adsorption on activated carbon. Langmuir 9:2758–2760. https://doi.org/10.1021/la00035a002

Chatterjee S, Rayalu S, Kolev SD, Krupadam RJ (2016) Adsorption of carbon dioxide on naturally occurring solid amino acids. J Environ Chem Eng 4(3):3170–3176. https://doi.org/10.1016/j.jece.2016.06.007

Choi HS, Suk MP (2009) Highly selective CO_2 capture in flexible 3D coordination polymer networks. Angew Chem Int Ed 48:6865–6869. https://doi.org/10.1002/anie.200902836

Drage TC, Smith KM, Arenillas A, Snape CE (2009) Developing strategies for the regeneration of polyethylenimine based CO_2 adsorbents. Energy Procedia 1:875–880. https://doi.org/10.1016/j.egypro.2009.01.116

Edenhofer O (2011) The IPCC special report on renewable energy sources and climate change mitigation. IPCC working group III "mitigation of climate change". The New School for Social Research, NY

Errahali M, Gatti G, Tei L, Paul G, Rolla GA, Canti L, Fraccarollo A, Cossi M, Comotti A, Sozzani P, Marchese L (2014) Microporous hyper-cross-linked aromatic polymers designed for methane and carbon dioxide adsorption. J Phys Chem C 118:28699–28710. https://doi.org/10.1021/jp5096695

Fontanals N, Marce RM, Borrull F, Cormack PAG (2015) Hypercrosslinked materials: preparation, characterization and applications. Polym Chem 6:7231–7244. https://doi.org/10.1039/C5PY00771B

Hudson MR, Queen WL, Mason JA, Fickel DW, Lobo RF, Brown CM (2012) Unconventional, highly selective CO_2 adsorption in zeolite SSZ-13. J Am Chem Soc 134:1970–1973. https://doi.org/10.1021/ja210580b

Jagiello J, Olivier JP (2009) A simple two-dimensional NLDFT model of gas adsorption in finite carbon pores: application to pore structural analysis. J Phys Chem C 113:19382–19385. https://doi.org/10.1021/jp9082147

Krupadam RJ, Korde BA, Ashokkumar M, Kolev SD (2014) Novel molecularly imprinted polymeric microspheres for preconcentration and preservation of polycyclic aromatic hydrocarbons from environmental samples. Anal Bioanal Chem 406(22):5313–5321. https://doi.org/10.1007/s00216-014-7952-z

Li B, Duan Y, Leuke D, Morreale B (2013) Advances in CO_2 capture technology: a patent review. Appl Energy 102:1439–1447. https://doi.org/10.1016/j.apenergy.2012.09.009

Liu S, Zhang Y, Jiang H, Wang X, Zhang T, Yao T (2018) High CO_2 capture by amino-modified bio-spherical cellulose nanofibres aerogels. Environ Chem Lett 16:605. https://doi.org/10.1007/s10311-017-0701-8

Lu W, Yuan D, Sculley J, Zhao D, Krishna R, Zhou HC (2011) Sulfonate-grafted porous polymer networks for preferential CO_2 adsorption at low pressure. J Am Chem Soc 133:18126–18129. https://doi.org/10.1021/ja2087773

Martin CF, Stockel E, Clowes R, Adams DJ, Cooper AI, Pis JJ, Rubiera F, Pevida C (2011) Hypercrosslinked organic polymer networks as potential adsorbents for pre-combustion CO_2 capture. J Mater Chem 21:5475–5483. https://doi.org/10.1039/c0jm03534c

McDonald JL, Sykora RE, Hixon P, Mirjafari A, Davis JH Jr (2014) Impact of water on CO_2 capture by amino acid ionic liquids. Environ Chem Lett 12:201. https://doi.org/10.1007/s13011-013-0435-1

Ohno K, Mandai Y, Matsuura H (1992) Vibrational spectra and molecular conformation of taurine and its related compounds. J Mol Struct 268:41–50. https://doi.org/10.1016/0022-2860(92)85058-O

Popp N, Homburg T, Stock N, Senker J (2015) Porous imine-based networks with protonated mine linkages for carbon dioxide separation from mixtures with nitrogen and methane. J Mater Chem A 3:18492–18504. https://doi.org/10.1039/C5TA02504D

Rabbani MG, Islamoglu T, El-Kaderi HM (2017) Benzothiazole-and benzoxazole-linked porous polymers for carbon dioxide storage and separation. J Mater Chem A 5:258–265. https://doi.org/10.1039/C6TA06342J

Salles G, Ghoufi A, Maurin G, Bell RG, Mellot-Draznieks C, Frey G (2008) Molecular dynamics simulations of breathing MOFs: structural transformations of MIL-53 (Cr) upon thermal activation and CO_2 adsorption. Angew Chem Int Ed 47:8487–8491. https://doi.org/10.1002/anie.200803067

Sekizkardes AK, Altarawneh S, Kahveci Z, Islamoğlu T, El-Kaderi HM (2014) Highly selective CO_2 capture by triazine-based benzimidazole-linked polymers. Macromolecules 47:8328–8334. https://doi.org/10.1021/ma502071w

Tan MXT, Zhang Y, Ying JY (2013) Mesoporous poly(melamine-formaldehyde) solid sorbent for carbon dioxide capture. Chem Sus Chem 6:1186–1190. https://doi.org/10.1002/cssc.201300107

Wahby A, Ramos-Fernandez JM, Martinez-Escandell M, Sepulveda-Escribano A, Silvestre-Albero J, Rodriguez-Reinoso F (2010) High surface area carbon molecular sieves for selective CO_2 adsorption. Chem Sus Chem 3:974–981. https://doi.org/10.1002/cssc.201000083

Walton KS, Snurr RQ (2007) Applicability of the BET method for determining surface areas of microporous metal–organic frameworks. J Am Chem Soc 129:8552–8556. https://doi.org/10.1021/ja071174k

Wilmer CE, Farha OK, Bae YS, Hupp JT, Snurr RQ (2012) Structure-property relationships fo porous materials for carbon dioxide separation and capture. Energy Environ Sci 5:9849–9856. https://doi.org/10.1039/C2EE23201D

Wulff G (1995) Molecular imprinting in cross-linked materials with the aid of molecular templates—a way towards artificial antibodies. Angew Chem Int Eds 34:1812–1832. https://doi.org/10.1002/anie.199518121

Xu C, Hedin N (2014) Microporous adsorbents for CO_2 capture—a case for microporous polymers. Mater Today 17:397–403. https://doi.org/10.1016/j.mattod.2014.05.007

Zhao Y, Shen Y, Bai L, Hao R, Dong L (2012) Synthesis and CO_2 adsorption properties of molecularly imprinted adsorbents. Environ Sci Technol 46:1789–1795. https://doi.org/10.1021/es203580b

Zhu X, Do-Thanh CL, Murdock CR, Nelson KM, Tian C, Brown S, Mahurin SM, Jenkins DM, Hu J, Zhao B, Liu H, Dai S (2013a) Efficient CO_2 capture by a 3D porous polymer derived from Troger's base. ACS Macro Lett 2:660–663. https://doi.org/10.1021/mz4003485

Zhu Y, Long H, Zhang W (2013b) Imine-linked porous polymer frameworks with high small gas (H_2, CO_2, CH_4, C_2H_2) uptake and CO_2/H_2 selectivity. Chem Mater 25:1630–1635. https://doi.org/10.1021/cm400019f